

Directed Gas-Phase Formation of Aminosilylene (HSiNH_2 ; X^1A'): The Simplest Silicon Analogue of an Aminocarbene, under Single-Collision Conditions

Zhenghai Yang, Chao He, Shane Goettl, Ralf I. Kaiser,* Valeriy N. Azyazov, and Alexander M. Mebel*



Cite This: *J. Am. Chem. Soc.* 2021, 143, 14227–14234



Read Online

ACCESS |



Metrics & More

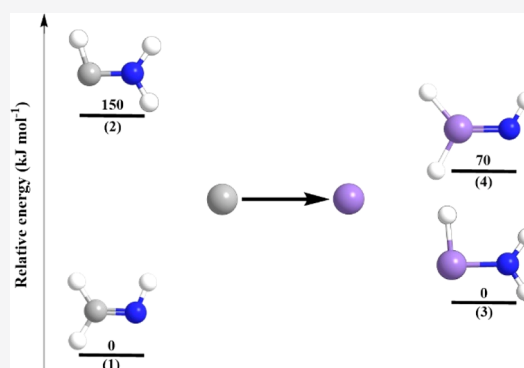


Article Recommendations



Supporting Information

ABSTRACT: The aminosilylene molecule (HSiNH_2 , X^1A')—the simplest representative of an unsaturated nitrogen-silylene—has been formed under single collision conditions via the gas phase elementary reaction involving the silyldyne radical (SiH) and ammonia (NH_3). The reaction is initiated by the barrierless addition of the silyldyne radical to the nonbonding electron pair of nitrogen forming an HSiNH_3 collision complex, which then undergoes unimolecular decomposition to aminosilylene (HSiNH_2) via atomic hydrogen loss from the nitrogen atom. Compared to the isovalent aminomethylene carbene (HCNH_2 , X^1A'), by replacing a single carbon atom with silicon, a profound effect on the stability and chemical bonding of the isovalent methanimine (H_2CNH)–aminomethylene (HNCH_2) and aminosilylene (HSiNH_2)–silanimine (H_2SiNH) isomer pairs is shown; i.e., thermodynamical stabilities of the carbene versus silylene are reversed by 220 kJ mol^{-1} . Hence, the isovalency of the main group XIV element silicon was found to exhibit little similarities with the atomic carbon revealing a remarkable effect not only on the reactivity but also on the thermochemistry and chemical bonding.



1. INTRODUCTION

In recent decades, the similarities and disparities between the carbon chemistries and the silicon chemistries have intrigued chemists with special attention devoted to the formation, chemical bonding, and electronic structure of carbenes (CRR') versus silylenes (SiRR') with R and R' representing (organic) substituents or hydrogen atoms.^{1,2} Carbenes are defined by a divalent carbon atom plus two unshared electrons resulting in an electron-deficient, six-electron valence shell.^{3,4} The simplest carbene—methylene (CH_2)—holds a triplet 3B_1 electronic ground state, and its first excited singlet state 1A_1 is higher by about 38 kJ mol^{-1} .^{5,6} Triplet carbenes have two unpaired electrons, whereas singlet carbenes are spin-paired and are characterized by an sp^2 hybridization of the carbon atom. With the exception of, for instance, the linear pentadiynylidene (HCCCCCH ; $X^3\Sigma_g^-$),⁷ most carbenes have a bent triplet ground state unless when bonded to a nitrogen, oxygen, sulfur, and/or halogen substituents. The latter donate an electron pair to the carbon atom empty p orbital at the carbene center thus stabilizing the singlet ground state. The singlet state will become the ground state if the energy is sufficiently reduced by the interaction of a nonbonding electron pair with the carbon atom empty p orbital.^{1,8} Overall, the electron sextet along with the coordinative unsaturation classifies gas phase carbenes as highly reactive transient species.⁹ However, the first report of an isolatable (phosphino)carbene [λ^3 -phosphinocarbene- λ^5 -

phosphaacetylene] by Bertrand et al.¹⁰ and of a stable N-heterocyclic carbene (NHC) [1,3-di(adamantyl)imidazol-2-ylidene] by Arduengo et al.¹¹ revolutionized the preparation of acyclic and N-heterocyclic carbenes with critical implications to metathesis catalysis and organo catalysis.^{12–14}

The isovalent silylenes can be formally derived from the silylene stem compound (SiH_2) by replacing the hydrogen atom(s) by substituents.¹⁵ Unlike carbenes, which do exist in triplet and singlet ground states, silylene derivatives hold exclusively singlet ground states with a lone (nonbonding) electron pair and empty 3p orbital centered at the silicon atom.^{16,17} Like carbenes, free gas phase silylenes have been classified as highly reactive and short-lived intermediates² until West and co-workers reported the first N-heterocyclic silylene (NHSi)—the isovalent class of N-heterocyclic carbene (NHC)—1,3-di-*tert*-butyl-2,3-dihydro-1*H*-1,3,2-diazasilol-2-ylidene stable at ambient temperature.¹⁸ This work stimulated extensive research into room temperature stable N-heterocyclic silylenes through the exploitation of the concept of kinetic

Received: May 28, 2021

Published: August 25, 2021



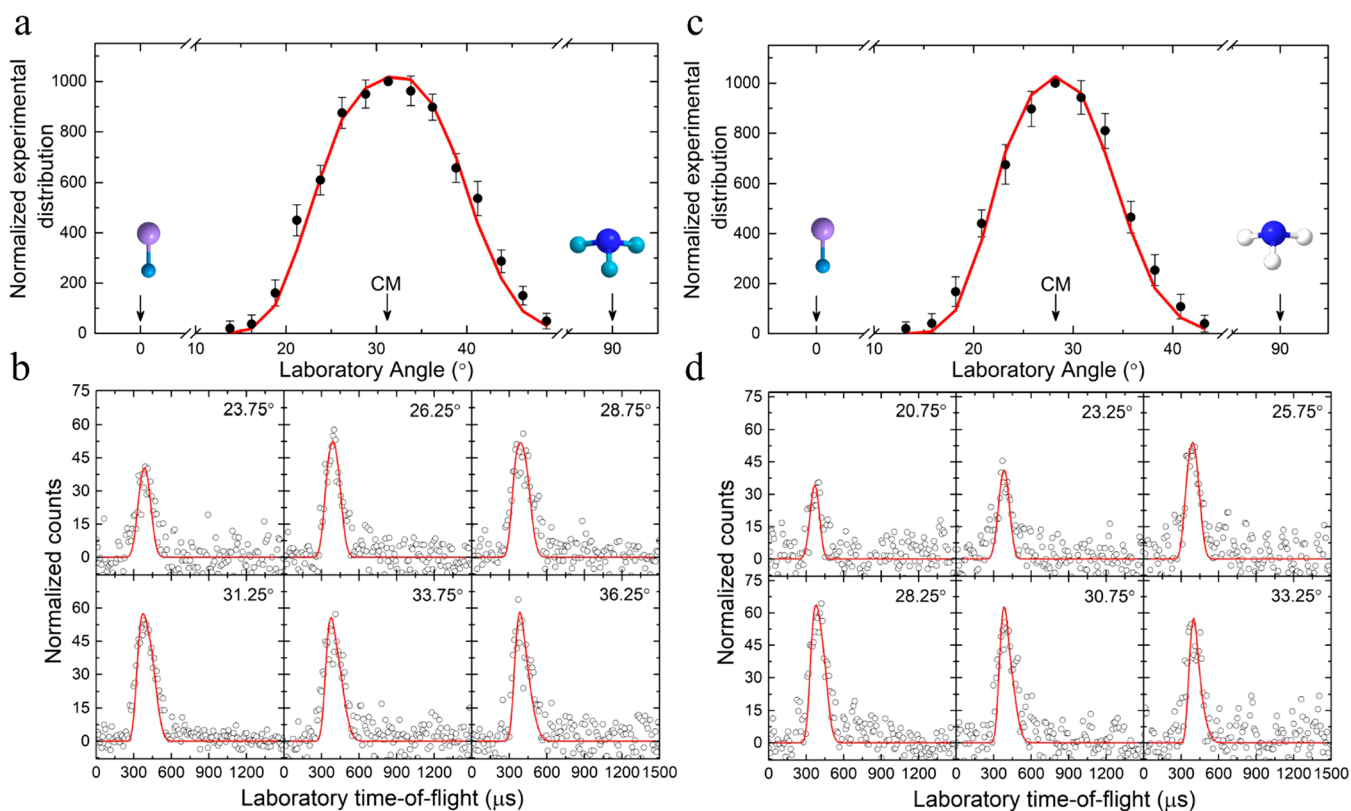


Figure 1. Laboratory angular distribution (a, c) and TOF spectra (b, d) for the reaction of the D1-silyldyne radical with D3-ammonia (data collected at $m/z = 48$ (a, b)) and with ammonia (data collected at $m/z = 46$ (c, d)). The solid circles define the experimental distribution; the open circles represent the experimental data; the red lines depict the best fits. Colors of the atoms: nitrogen, blue; silicon, purple; hydrogen, white; deuterium, light blue.

stabilization through sterically hindered substituents like bulky alkyl groups at the nitrogen atom in the ring along with electronic stabilization through nitrogen lone pair π -donation into the empty 3p orbital at the divalent silicon.¹⁹ Recently, stable acyclic silylenes were synthesized by Rekker et al. with a S–Si–S angle of 90.52° along with a HOMO–LUMO gap of 411 kJ mol^{-1} and by Protchenko et al. with a HOMO–LUMO gap of 197 kJ mol^{-1} together with a B–Si–N angle of 109.7° .^{20,21}

However, despite the impressive progress in preparing stable acyclic and *N*-heterocyclic silylenes, little attention was devoted to the directed gas phase formation and characterization of the simplest unsaturated nitrogen-silylene aminosilylene (HSiNH_2 ; X^1A'). Aminosilylene has previously been detected using argon matrix at 12 K after photolysis of silyl azide (H_3SiN_3)²² and mixing ablated silicon atoms with ammonia,²³ the mechanism involving the formation of aminosilylene was proposed by Beach et al. via laser-induced photochemistry of silane (SiH_4)–ammonia (NH_3) mixtures.²⁴ In 2010, rotational spectra of aminosilylene were preliminarily studied within the discharge of silane–ammonia mixtures.²⁵ Since a unified picture of the underlying gas phase chemistry and chemical bonding of the isovalent imines and aminocarbenes such as methanimine (H_2CNH ; $^1A'$) and aminomethylene (HCNH_2 ; $^1A'$) is beginning to emerge,^{26–29} as the silicon isovalent counterpart of an aminocarbene, free gas phase aminosilylene (HSiNH_2 ; X^1A') represents the simplest, but least explored representative of a key class of silicon-bearing reactive intermediates due to its high reactivity and inherent short lifetime. Here, we provide an exceptional peak

into the elusive gas phase formation of aminosilylene (HSiNH_2 ; X^1A')—the simplest silicon analogues of aminocarbene—via the elementary reaction of the D1-silyldyne radical (SiD ; $X^2\Pi$) with D3-ammonia (ND_3 ; X^1A_1) and ammonia (NH_3 ; X^1A_1) under single collision conditions exploiting crossed molecular beam experiments merged with electronic structure calculations. The studies are conducted at the most microscopic and fundamental level, shedding light on the underlying reaction mechanisms leading to a clean gas phase formation of the simplest aminosilylene *without* successive reactions thus providing new insights on the underlying reaction dynamics of one of the most elusive representatives of a rather obscure class of highly reactive silylenes: aminosilylene (HSiNH_2 ; X^1A').

2. RESULTS

2.1. Laboratory Frame. Considering the inherent background of $^{12}\text{CO}_2^+$ and $^{13}\text{CO}_2^+$ in the detector, data at $m/z = 44$ and 45 cannot be detected. To explore both atomic deuterium and molecular deuterium loss channels, fully deuterated reactants (SiD-ND_3) are employed first. For the SiD (30 amu)– ND_3 (20 amu) reaction, a reactive scattering signal was observed at $m/z = 48$ ($^{28}\text{SiND}_3^+$, $^{30}\text{SiND}_2^+$) and 46 ($^{28}\text{SiND}_2^+$, $^{30}\text{SiND}^+$) with signal at $m/z = 46$ accumulated at a $37 \pm 3\%$ level compared to $m/z = 48$. Considering the silicon natural isotope abundances (^{28}Si (92.2%), ^{29}Si (4.7%), ^{30}Si (3.1%)) and that the time-of-flight (TOF) spectra of $m/z = 48$ and 46 are identical after scaling, we conclude that a single reaction channel exists in the experiment, i.e., the reaction of D1-silyldyne (SiD , 30 amu) with D3-ammonia (ND_3 , 20 amu)

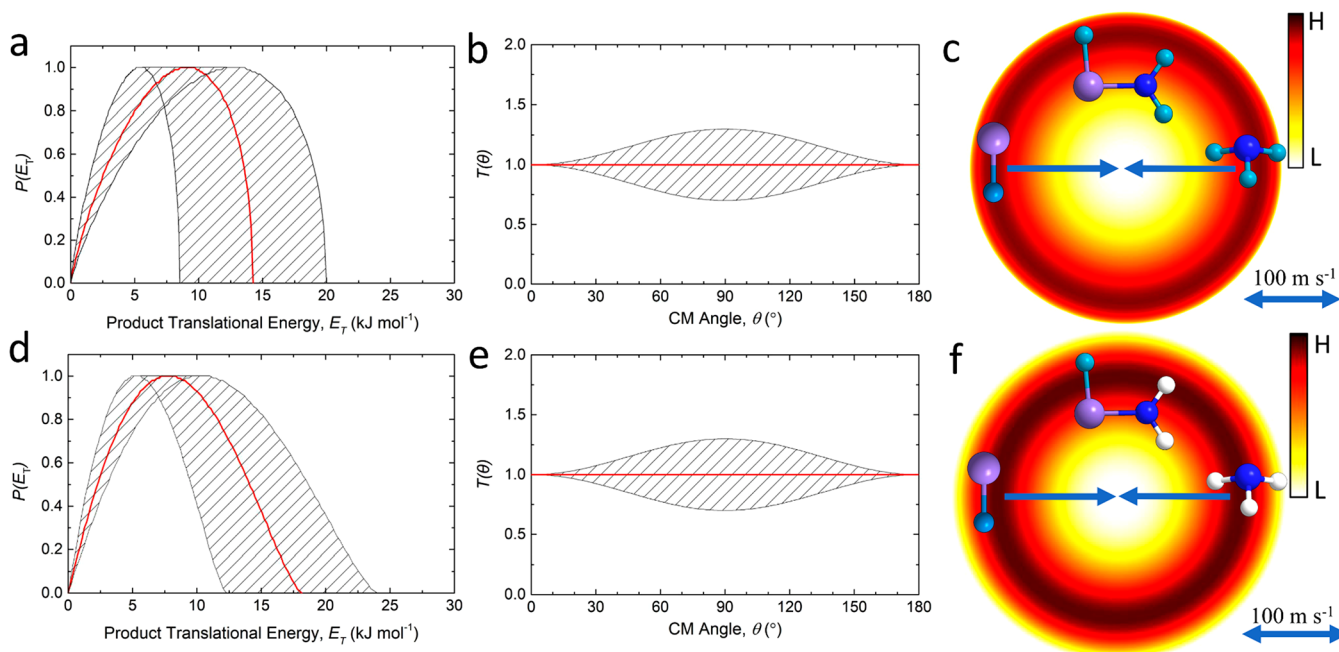
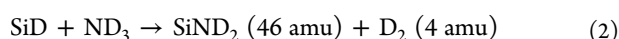
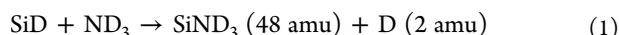


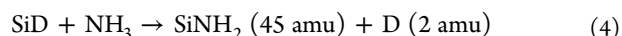
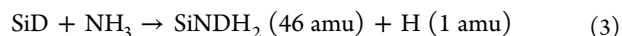
Figure 2. Center-of-Mass translational energy (a, d), angular flux distributions (b, e) and the corresponding flux contour map (c, f) for the reaction of D1-silyldiyne with D3-ammonia (data collected at $m/z = 48$ (a, b, c)) and with ammonia (data collected at $m/z = 46$ (d, e, f)). The red lines represent the best-fit; shaded areas depict the error limits of the best fits.

forming SiND₃ (48 amu) along with atomic deuterium (D, 2 amu) (reaction 1). The signal at $m/z = 46$ originates from dissociative electron impact ionization of parent SiND₃ product in the ionizer, but due to the overlapping TOFs at $m/z = 48$ and 46 not from the molecular deuterium loss (reaction 2). No ion counts were detected at $m/z = 50$ (²⁸SiND₄⁺, ³⁰SiND₃⁺) and 49 (²⁹SiND₃⁺); these findings suggest that no ²⁸SiND₄ adducts survive the flight time of 411 μs from the collision center to the ionization region of the detector and that neither ²⁹Si- nor ³⁰Si-substituted SiND₃ isotopologues were formed in sufficient high yields to be detected under our experimental conditions. Consequently, the laboratory data alone reveal that SiND₃ isomer(s) are formed via the elementary reaction of the D1-silyldiyne with D3-ammonia through the D1-silyldiyne versus atomic deuterium exchange pathway (reaction 1). The angular resolved TOF spectra were then accumulated at $m/z = 48$ and scaled to the TOF recorded at the center-of-mass angle to yield the laboratory angular distribution (LAD). The latter distribution spreads 35° within the scattering plane and shows a maximum at the CM angle (Figure 1). The nearly forward–backward symmetry with regard to the CM angle of the distribution suggests indirect reaction dynamics involving SiND₄ reaction intermediate(s).³⁰ It is important to stress that the quadrupole mass spectrometer works in time-of-flight mode; i.e., this device records the flight time of a product molecule at a well-defined mass-to-charge ratio from the interaction region to the electron impact ionizer. Our instrument does not record classical mass spectra of the formed products.



In a fully deuterated SiD-ND₃ reaction, atomic deuterium can be emitted from the D1-silyldiyne and/or from D3-ammonia reactant(s). For more information, the reaction of

D1-silyldiyne (SiD, 20 amu) with ammonia (NH₃, 17 amu) was also explored (Figure 1; reactions 3 and 4). The signal at $m/z = 46$ should originate from the hydrogen atom loss from the ammonia reactant (reaction 3); two loss channels can contribute to signal at $m/z = 45$: atomic deuterium loss from the D1-silyldiyne reactant in reaction 4 and dissociative electron impact ionization of the hydrogen atom loss product (SiNDH₂) of reaction 3. In the experiment, the scattering signal was observed at $m/z = 46$; background interference from ¹³CO₂⁺ ($m/z = 45$) prevented detection of reaction 4. Therefore, in the SiD-NH₃ reaction, the hydrogen atom originated at least from the ammonia reactant leading to SiNDH₂. Similar to the D1-silyldiyne–D3-ammonia system, the resulting LAD for the D1-silyldiyne–ammonia system is also forward–backward symmetric with regard to the CM angle; compared to the ejected deuterium atom (reaction 1), the lighter hydrogen atom (reaction 3) leads to the narrower LAD distribution for the D1-silyldiyne–ammonia reaction (spans only 30° within the scattering plane).



2.2. Center-of-Mass Frame. To elucidate the nature of the SiND₃ and SiNDH₂ isomers formed via the atomic deuterium and hydrogen losses, respectively, the laboratory data were transformed into a CM reference frame. This procedure yields two distributions, i.e., the CM translational energy $P(E_T)$ and angular $T(\theta)$ flux distribution.^{31,32} In both systems, the laboratory data could be fit with a single channel, i.e., D loss channel (SiND₃ (48 amu) plus D (2 amu); reaction 1) and H loss channel (SiNDH₂ (46 amu) plus H (1 amu); reaction 3) (Figure 2). In detail, for products formed without internal excitation, considering the law of energy conservation, the maximum translational energy (E_{max}) of $14 \pm 6 \text{ kJ mol}^{-1}$ and $18 \pm 6 \text{ kJ mol}^{-1}$, which can be derived from the $P(E_T)$,

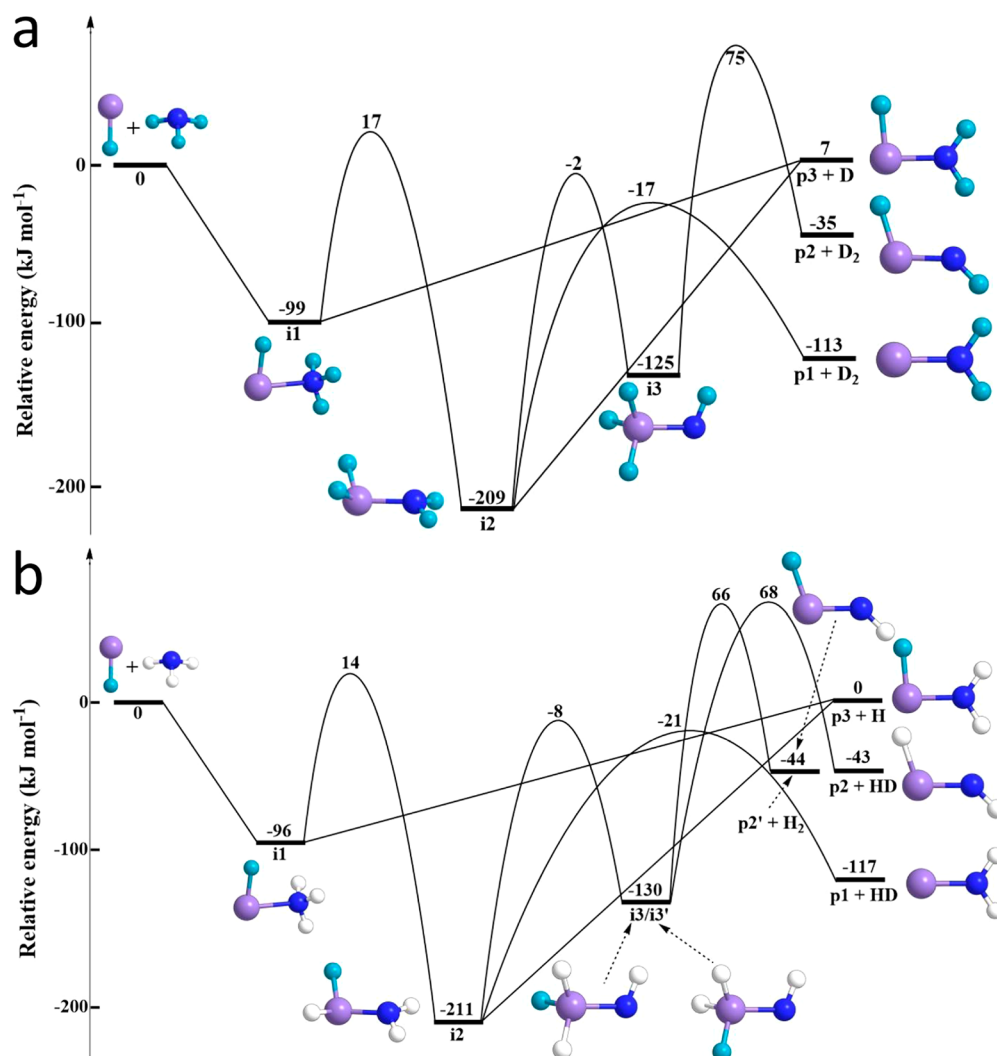


Figure 3. Potential energy surface (PES) for the reaction of the D1-silyldyne radical with D3-ammonia (a) and with ammonia (b). A complete PES is presented in Figure S1. Colors of the atoms: nitrogen, blue; silicon, purple; hydrogen, white; deuterium, light blue.

represents the sum of the reaction exoergicity and the collision energy ($15.9 \pm 0.4 \text{ kJ mol}^{-1}$; $14.9 \pm 0.4 \text{ kJ mol}^{-1}$). This suggests that the SiD-ND₃ and SiD-NH₃ reactions are essentially thermo neutral within the error limits ($2 \pm 6 \text{ kJ mol}^{-1}$; $-3 \pm 6 \text{ kJ mol}^{-1}$).

Further, the $P(E_T)$ distribution peak at $9 \pm 3 \text{ kJ mol}^{-1}$ and $8 \pm 2 \text{ kJ mol}^{-1}$ suggest rather loose exit transition states together with simple bond rupture processes forming upon decomposition of the reaction intermediates via atomic deuterium and hydrogen loss, respectively. Finally, in both systems, the CM angular distributions reveal nonzero intensity from 0° to 180° along with a forward-backward symmetry. These findings provide compelling evidence of indirect reaction dynamics involving long-lived SiND₄ and SiNDH₃ intermediate(s), holding lifetime longer than their rotational periods.^{30,33} These findings are also reflected in the flux contour maps, which depict the reactive scattering products flux intensity as a function of the CM scattering angle and product velocity, containing the information on the reactive scattering process.³⁰

3. DISCUSSION

Having proved the gas phase formation of the SiND₃ isomer(s) in the SiD-ND₃ system and of SiNDH₂ isomer(s) in the SiD-

NH₃ system, we are now merging the electronic structure calculations with experimental results to untangle the nature of the product isomer(s) formed and the underlying reaction mechanisms. The accurate electronic structure calculations were conducted with the relative energies of the local minima, and transition states are predicted within 8 kJ mol^{-1} and the overall reaction energies within 3 kJ mol^{-1} (Figure 3; Figure S1). The electronic structure calculations identified four SiNH₃ (**p3**, **p4**, **p6**, **p7**) and three SiNH₂ isomers (**p1**, **p2**, **p5**) formed via atomic and molecular hydrogen loss, respectively. Among the atomic hydrogen loss products, aminosilylene (HSiNH₂, **p3**, C_s , X^1A') represents the most stable isomer followed by silanimine (H₂SiNH, **p4**, C_s , X^1A'), silyldyneammonia (SiNH₃, **p6**, C_{3v} , X^3A_1), and imidogensilyl (H₃SiN, **p7**, C_{3v} , X^3A_1). The overall reaction energies of 2, 72, 196, and 281 kJ mol^{-1} reveal that, under a collision energy of 15 kJ mol^{-1} , only aminosilylene (HSiNH₂, **p3**, C_s , X^1A') is energetically accessible. With respect to the molecular hydrogen loss channel, the doublet radicals aminosilyldyne (SiNH₂, **p1**, C_{2v} , X^2B_2), imidogensilylene (HSiNH, **p2**, C_s , X^2A'), and imidogensilyl (H₂SiN, **p5**, C_{2v} , X^2B_2) can be formed in bimolecular reactions with reaction energies of -117 , -43 , and $+90 \text{ kJ mol}^{-1}$, respectively. The relative energies of the

products are in excellent agreement with earlier computational studies.^{23,34,35} These data reveal that imidogensilyl (H_2SiN , **p5**, C_{2v} , X^2B_2) is energetically not accessible. Therefore, the consecutive discussion centers on the channels forming **p1** to **p3**.

For the SiD-ND₃ system, the calculations reveal that the D1-silyliidyne radical (SiD) adds barrierlessly to the nonbonding electron pair of nitrogen forming a silicon–nitrogen single bond (212.2 pm) and the initial collision complex **i1** on the doublet surface (Figure 3). All attempts to locate insertion pathways of D1-silyliidyne into the nitrogen–deuterium bond to intermediate **i2** failed and resulted in intermediate **i1**. Intermediate **i1** can isomerize to intermediate **i2**, which represents the global minimum of the SiND₄ potential energy surface (PES), through a barrier located 17 kJ mol⁻¹ above the separated reactants. Alternatively, the initial collision complex can undergo unimolecular decomposition to D3-aminosilylene (DSiND₂, **p3**, C_s , X^1A'), i.e., the thermodynamically most stable SiND₃ isomer. Intermediate **i2** can undergo unimolecular decomposition to D2-aminosilyliidyne (SiND₂, **p1**, C_{2v} , X^2B_2) through molecular deuterium loss or to D3-aminosilylene (DSiND₂, **p3**, C_s , X^1A') via atomic deuterium loss. Intermediate **i2** can also isomerize via a deuterium shift to **i3**, which then emits molecular deuterium yielding D2-imidogensilylene (DSiND, **p2**, C_s , X^2A'). The experimental collision energy of 15.9 ± 0.4 kJ mol⁻¹ is slightly lower than the isomerization barrier of **i1** (DSiND₃, C_s , X^2A'') → **i2** (D₂SiND₂, C_s , X^2A'). If intermediate **i2** is formed, unimolecular decomposition of the latter should result in a molecular deuterium loss (forming **p1** and/or **p2**)—which was experimentally not observed—as well as atomic deuterium loss (forming **p3**). On the other hand, atomic deuterium loss from **i1** could yield exclusively D3-aminosilylene (DSiND₂, **p3**, C_s , X^1A'). Based on the aforementioned considerations, the reaction dynamics are indirect through the involvement of SiND₄ complexes and initiated by the barrierless addition of D1-silyliidyne to the nonbonding electron pair of D3-ammonia forming **i1** (DSiND₃, C_s , X^2A''), which then eliminated a deuterium atom from the nitrogen atom yielding the thermodynamically most stable SiND₃ isomer D3-aminosilylene (DSiND₂, **p3**, C_s , X^1A'). The lack of any molecular deuterium product channel suggests that the barrier to isomerization from **i1** to **i2** cannot be overcome, a conclusion which is in line with the computed barrier of 17 kJ mol⁻¹, which is slightly higher than the collision energy in our experiments. The computed reaction energy of $+7 \pm 3$ kJ mol⁻¹ forming D3-aminosilylene (**p3**) agrees very well with the experimental reaction energy of $+2 \pm 6$ kJ mol⁻¹. These conclusions are also supported by the SiD-NH₃ system (Figure 3). Here, the atomic hydrogen loss from **i1**—also formed via barrierless addition of the D1-silyliidyne radical to ammonia—leads to D1-aminosilylene (DSiNH₂, **p3**, C_s , X^1A') in a thermoneutral reaction, which matches the experimental reaction energy of -3 ± 6 kJ mol⁻¹.

Overall, the crossed molecular beam experiments merged with electronic structure calculations provide compelling evidence on the first directed gas phase formation of D3- and D1-aminosilylene (DSiND₂/DSiNH₂, **p3**, C_s , X^1A') under single collision conditions.

The thermodynamical differences in the stability between carbene and silylene are reflected by comparing the aminosilylene with the isovalent aminomethylene (HCNH₂) molecules. The profound effect by replacing a single carbon

atom by silicon is depicted in Figure 4. The molecular geometries of methanimine (**1**) and aminomethylene (**2**) including the relative energies, bond distances, and angles were extracted from the literature.^{36–39}

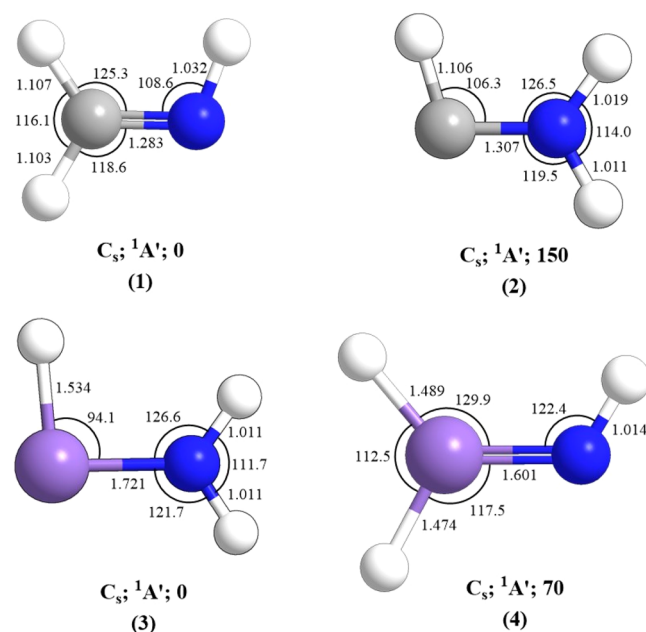


Figure 4. Geometries, point groups, electronic ground state wave functions, relative energies (kJ mol⁻¹), bond distances (Å), and selected bond angles (degrees) of methanimine (**1**, H_2CNH) and aminomethylene (**2**, HCNH_2) along with their isovalent species of aminosilylene (**3**, HSiNH_2) and silanimine (**4**, H_2SiNH). Colors of the atoms: nitrogen, blue; silicon, purple; carbon, gray; hydrogen, white.

4. CONCLUSIONS

Our combined experimental and theoretical study provides compelling evidence of the directed gas phase formation of aminosilylene (HSiNH_2 ; **p3**)—the simplest silicon analogue of an aminocarbene—under single collision conditions, via the silyliidyne (SiH)-ammonia (NH_3) reaction. Initially, the barrierless addition of the silyliidyne radical to the nonbonding electron pair of nitrogen will lead to an HSiNH_3 collision complex, which then undergoes unimolecular decomposition to aminosilylene (HSiNH_2 ; **p3**) via atomic hydrogen loss from the nitrogen atom. The distinct chemical bondings of silicon–nitrogen versus the isovalent carbon–nitrogen compounds are well expressed, when contemplating aminosilylene (**3**) and silanimine (**4**) with their carbon analogues methanimine (**1**) and aminomethylene (**2**) (Figure 4).^{34,36–40} Methanimine (H_2CNH , **1**) represents the global minimum and is thermodynamically more stable by 150 kJ mol⁻¹ compared to the carbene structure aminomethylene (HCNH_2 , **2**). The sequence of stability is reversed when replacing a carbon atom by silicon with aminosilylene (HSiNH_2 , **3**) corresponding to the global minimum and silanimine (H_2SiNH , **4**) lying 70 kJ mol⁻¹ higher in energy. The enhanced stability of **3** compared to **4** can be rationalized through a favorable π -type back-donation of the nonbonding electron pair of nitrogen into the empty p_z orbital at the silicon atom; this in turn stabilizes the silylene structure (**3**) and results in a close to 90° hydrogen–silicon–nitrogen angle, i.e. no hybridization of the silicon

atom, whereas the sp^2 -hybridized carbon atom in aminomethylene (2) is consistent with the hydrogen–carbon–nitrogen angle of 106° . This electronic structure of aminosilylene is illustrated by its molecular orbitals shown in Figure 5; for instance, the HOMO–1 corresponds to the π -type back-

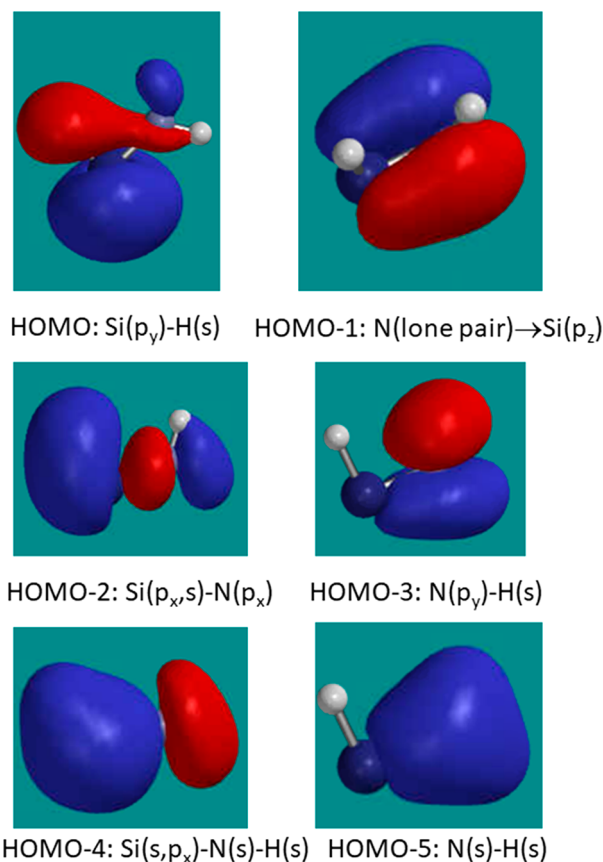


Figure 5. Valence molecular orbitals of aminosilylene (HSiNH_2 , 3).

donation from nitrogen to silicon. The absence of hybridization between the s and p orbitals of the silicon atoms is also clearly evident (Figure 5). Overall, as the silicon analogue of the simplest aminocarbene, aminomethylene (2), aminosilylene (3) represents a previously elusive key reaction intermediate in the gas phase inorganic silicon chemistry revealing that crossed molecular beam experiments carry advantages such as a gas phase formation of aminosilylene (HSiNH_2). This species represents a benchmark of one of the most elusive representatives of a rather obscure class of highly reactive silylenes, which can be formed in gas phase with the primary reaction products “flying away” undisturbed *without* successive reactions. This clean bimolecular gas phase reaction might represent a universal template toward the formation of even substituted aminosilylenes (HSiNHR) with R being an organic group through reactions of silylydine radicals with primary amines (NH_2R) thus shedding light on the previously obscure chemistry of aminosilylenes.

5. EXPERIMENTAL AND COMPUTATIONAL

5.1. Experimental Section. The reaction of the D1-silylydine radical (SiD ; $X^2\Pi$) with D3-ammonia (ND_3 ; X^1A_1) and ammonia (NH_3 ; X^1A_1) were conducted exploiting a crossed molecular beams machine.⁴¹ The D1-silylydine pulsed supersonic beam was formed *in situ* in the primary chamber by laser ablation of a rotating silicon rod

with 266 nm pulses (4–8 mJ per pulse; 30 Hz) and entrainment of the ablated species in a 1:1 mixture of deuterium gas (D_2 , >99.7%; Linde) and neon (Ne ; 99.999%; Matheson) released by a pulsed piezoelectric valve with 4 atm backing pressure, 60 Hz repetition rate.⁴² The D1-silylydine beam was optimized at a unique mass-to-charge value of $m/z = 31$ ($^{29}\text{SiD}^+$) for intensity, considering the natural silicon isotope abundances (^{28}Si (92.2%), ^{29}Si (4.7%), ^{30}Si (3.1%)). The primary D1-silylydine beam was first skimmed and then velocity-selected by a high stable four-slot chopper wheel (120 Hz) controlled by a precision motion system.⁴² The chopped section of the D1-silylydine beam is defined by a peak velocity (v_p) of 1200 m s^{-1} and speed ratio (S) of 6 (Table S1). It should be noted that no higher molecular weight silicon-deuterium bearing species were detected in the primary beam in the experiment. Considering the $18 \mu\text{s}$ travel time from the ablation to the interaction region along with a lifetime of 500 ns for electronically excited $A^2\Delta$ of D1-silylydine, potentially excited D1-silylydine radicals should relax to their ground state.⁴³ The primary beam crossed perpendicularly with the secondary D3-ammonia (ND_3 ; Sigma-Aldrich; 99% D) or ammonia (NH_3 ; Matheson; 99.99%) beam released by a pulsed piezo valve with a backing pressure of 550 Torr. The velocities of the crossing segment of the secondary beams as compiled in Table S1 resulted in collision energies (E_C) of $15.9 \pm 0.4 \text{ kJ mol}^{-1}$ for the SiD-ND_3 and $14.9 \pm 0.4 \text{ kJ mol}^{-1}$ for the SiD-NH_3 reaction, respectively. Reactively scattering products were ionized by an electron impact ionizer (80 eV, 2 mA), mass filtered according to distinct mass-to-charge ratios (m/z) exploiting a quadrupole mass spectrometer (Extrel, QC 150), and ultimately recorded by a Daly type ion counter.^{44,45} The detector assembly is located in a differentially pumped ultrahigh vacuum (UHV) chamber operated routinely at 7×10^{-12} Torr. The recorded laboratory data were transformed into the CM reference frame to obtain reaction dynamics information using a forward-convolution routine.^{32,46,47} User-defined CM angular $T(\theta)$ and translational energy $P(E_T)$ flux distributions are optimized until a best fit of the laboratory frame angular distribution and TOF spectra is achieved. The reactive differential cross section $I(u, \theta) \approx P(u) \times T(\theta)$ is then derived with the velocity u and CM angle θ .

5.2. Computational. We employed density functional theory (DFT) within the frame of the hybrid B3LYP^{48,49} method and with the 6-311G(d,p) basis set to optimize the geometric structures of the reactants, products, intermediates, and transition states taking part in the reaction of silylydine with ammonia. Next, the same B3LYP/6-311G(d,p) method was used to compute vibrational frequencies of all stationary structures, while considering the particular isotopic composition of the $^{28}\text{Si}^{14}\text{ND}_x\text{H}_{4-x}$ species involved in the $\text{SiH} + \text{NH}_3/\text{SiD} + \text{ND}_3/\text{SiD} + \text{NH}_3$ reactions. For the reactants and the critical transition state for the H atom migration **i1**–**i2**, geometry optimization was also carried out at the doubly hybrid DFT B2PLYPD3/6-311G(d,p) level of theory^{50,51} with a dispersion correction⁵² and at the coupled clusters CCSD/6-311G(d,p) level.^{53–56} For the B2PLYPD3/6-311G(d,p) optimized structures, vibrational frequencies were recalculated using the same method. Further refinement of single-point energies was performed at the explicitly correlated coupled clusters CCSD(T)-F12 level^{57,58} with single and double excitations and perturbative treatment of triple excitations, with the cc-pVQZ-f12 basis set⁵⁹ for most structures. Additionally, for the reactants and the critical **i1**–**i2** transition state, the calculations were also carried out with the cc-pVTZ-f12 basis set, and then, the energies were extrapolated to the complete basis set (CBS) limit using the two-point formula, $E_{\text{CBS}} = E_{\text{cc-pVQZ-f12}} + (E_{\text{cc-pVQZ-f12}} - E_{\text{cc-pVTZ-f12}}) \times 0.69377$.⁶⁰ For the critical species, the CCSD(T)-F12/CBS energies were evaluated at three different optimized geometries obtained with B3LYP, B2PLYPD3, and CCSD. Moreover, to incorporate the core electron correlation effects, the energies of these species were further improved using CCSD-(full,T)-F12 calculations, which included, when handling the electronic correlation, all core electrons except 1s of Si atoms, with the cc-pCVTZ-f12 and cc-pCVQZ-f12 basis sets⁶¹ and extrapolated to the CBS limit. Calculations of anharmonic frequencies were executed at the B3LYP/6-311G(d,p) level using vibrational perturbation theory

to the second order (VPT2)⁶² with the goal to assess anharmonicity corrections to zero-point vibrational energies. The GAUSSIAN 09 package⁶³ was employed for all B3LYP and B2PLYPD3 calculations as well as CCSD geometry optimizations and VPT2 computations of anharmonic frequencies. Alternatively, the MOLPRO 2010 package⁶⁴ was utilized for the CCSD(T)-F12 calculations. Noteworthy, the CCSD(T)-F12/CBS relative energies of the i1–i2 transition state including the core correlation and anharmonic ZPE corrections with its geometry optimized using all three different methods agreed with its CCSD(T)-F12/cc-pVQZ-f12//B3LYP/6-311G(d,p) + ZPE-(B3LYP/6-311G(d,p)) energy with harmonic ZPE in the margins of 1–2 kJ mol⁻¹.

■ ASSOCIATED CONTENT

SI Supporting Information

The Supporting Information is available free of charge at <https://pubs.acs.org/doi/10.1021/jacs.1c05510>.

Experimental details of Si–NH₃/ND₃ reactions, complete potential energy diagram (Figure S1), the experimental parameters (Table S1), optimized geometric structures in the form of Cartesian coordinates and vibrational frequencies for all stationary structures involved in the reactions (Table S2) (PDF)

■ AUTHOR INFORMATION

Corresponding Authors

Ralf I. Kaiser – Department of Chemistry, University of Hawai'i at Manoa, Honolulu, Hawaii 96822, United States; orcid.org/0000-0002-7233-7206; Email: ralfk@hawaii.edu

Alexander M. Mebel – Department of Chemistry and Biochemistry, Florida International University, Miami, Florida 33199, United States; orcid.org/0000-0002-7233-3133; Email: mebela@fiu.edu

Authors

Zhenghai Yang – Department of Chemistry, University of Hawai'i at Manoa, Honolulu, Hawaii 96822, United States
Chao He – Department of Chemistry, University of Hawai'i at Manoa, Honolulu, Hawaii 96822, United States
Shane Goettl – Department of Chemistry, University of Hawai'i at Manoa, Honolulu, Hawaii 96822, United States
Valeriy N. Azyazov – Lebedev Physical Institute, Samara 443011, Russian Federation

Complete contact information is available at: <https://pubs.acs.org/doi/10.1021/jacs.1c05510>

Notes

The authors declare no competing financial interest.

■ ACKNOWLEDGMENTS

This work at the University of Hawaii was supported by the U.S. National Science Foundation (CHE-1853541). Ab initio calculations at Lebedev Physics Institute in Samara were supported by the Ministry of Science and Higher Education of the Russian Federation via Grant No. 075-15-2021-597.

■ REFERENCES

- (1) Bourissou, D.; Guerret, O.; Gabbai, F. P.; Bertrand, G. Stable Carbenes. *Chem. Rev.* **2000**, *100*, 39–92.
- (2) Driess, M. Breaking the Limits with Silylenes. *Nat. Chem.* **2012**, *4*, 525–526.

- (3) Buchner, E.; Curtius, T. Ueber die Einwirkung von Diazoessigäther auf aromatische Kohlenwasserstoffe. *Ber. Dtsch. Chem. Ges.* **1885**, *18*, 2377–2379.

- (4) Staudinger, H.; Kupfer, O. Über reaktionen des methylen. III. Diazomethan. *Ber. Dtsch. Chem. Ges.* **1912**, *45*, 501–509.

- (5) Sander, W.; Bucher, G.; Wierlacher, S. Carbenes in Matrixes: Spectroscopy, Structure, and Reactivity. *Chem. Rev.* **1993**, *93*, 1583–1621.

- (6) Comeau, D. C.; Shavitt, I.; Jensen, P.; Bunker, P. R. An Ab Initio Determination of the Potential-Energy Surfaces and Rotation–Vibration Energy Levels of Methylene in the Lowest Triplet and Singlet States and the Singlet–Triplet Splitting. *J. Chem. Phys.* **1989**, *90*, 6491–6500.

- (7) He, C.; Galimova, G. R.; Luo, Y.; Zhao, L.; Eckhardt, A. K.; Sun, R.; Mebel, A. M.; Kaiser, R. I. A Chemical Dynamics Study on the Gas-Phase Formation of Triplet and Singlet C₃H₂ Carbenes. *Proc. Natl. Acad. Sci. U. S. A.* **2020**, *117*, 30142–30150.

- (8) Irikura, K. K.; Goddard III, W. A.; Beauchamp, J. L. Singlet–Triplet Gaps in Substituted Carbenes CX₂ (X, Y = H, F, Cl, Br, I, SiH₃). *J. Am. Chem. Soc.* **1992**, *114*, 48–51.

- (9) Hopkinson, M. N.; Richter, C.; Schedler, M.; Glorius, F. An Overview of N-Heterocyclic Carbenes. *Nature* **2014**, *510*, 485–496.

- (10) Igau, A.; Grutzmacher, H.; Baceiredo, A.; Bertrand, G. Analogous α,α' -Bis-Carbenoid Triply Bonded Species: Synthesis of a Stable λ^3 -Phosphinocarbene- λ^5 -Phosphaacetylene. *J. Am. Chem. Soc.* **1988**, *110*, 6463–6466.

- (11) Arduengo, A. J., III; Harlow, R. L.; Kline, M. A Stable Crystalline Carbene. *J. Am. Chem. Soc.* **1991**, *113*, 361–363.

- (12) Raoufmoğhaddam, S.; Zhou, Y.-P.; Wang, Y.; Driess, M. N-Heterocyclic Silylenes as Powerful Steering Ligands in Catalysis. *J. Organomet. Chem.* **2017**, *829*, 2–10.

- (13) Dröge, T.; Glorius, F. The Measure of All Rings—N-Heterocyclic Carbenes. *Angew. Chem., Int. Ed.* **2010**, *49*, 6940–6952.

- (14) Enders, D.; Niemeier, O.; Henseler, A. Organocatalysis by N-Heterocyclic Carbenes. *Chem. Rev.* **2007**, *107*, 5606–5655.

- (15) Haaf, M.; Schmedake, T. A.; West, R. Stable Silylenes. *Acc. Chem. Res.* **2000**, *33*, 704–714.

- (16) Takahashi, S.; Ishii, A.; Nakata, N. Interconversion between a Silamine and an Aminosilylene Supported by an Iminophosphonamide Ligand. *Chem. Commun.* **2021**, *57*, 3203–3206.

- (17) Kovačević, G.; Pivac, B. Reactions in Silicon–Nitrogen Plasma. *Phys. Chem. Chem. Phys.* **2017**, *19*, 3826–3836.

- (18) Denk, M.; Lennon, R.; Hayashi, R.; West, R.; Belyakov, A. V.; Verne, H. P.; Haaland, A.; Wagner, M.; Metzler, N. Synthesis and Structure of a Stable Silylene. *J. Am. Chem. Soc.* **1994**, *116*, 2691–2692.

- (19) Asay, M.; Jones, C.; Driess, M. N-Heterocyclic Carbene Analogues with Low-Valent Group 13 and Group 14 Elements: Syntheses, Structures, and Reactivities of a New Generation of Multitalented Ligands. *Chem. Rev.* **2011**, *111*, 354–396.

- (20) Protchenko, A. V.; Birjkumar, K. H.; Dange, D.; Schwarz, A. D.; Vidovic, D.; Jones, C.; Kaltsoyannis, N.; Mountford, P.; Aldridge, S. A Stable Two-Coordinate Acyclic Silylene. *J. Am. Chem. Soc.* **2012**, *134*, 6500–6503.

- (21) Rekker, B. D.; Brown, T. M.; Fettinger, J. C.; Tuononen, H. M.; Power, P. P. Isolation of a Stable, Acyclic, Two-Coordinate Silylene. *J. Am. Chem. Soc.* **2012**, *134*, 6504–6507.

- (22) Maier, G.; Glatthaar, J.; Reisenauer, H. P. Hetero- π -Systeme. XVII: Aminosilylen (Aminosilandiyl). *Chem. Ber.* **1989**, *122*, 2403–2405.

- (23) Chen, M.; Zheng, A.; Lu, H.; Zhou, M. Reactions of Atomic Silicon and Germanium with Ammonia: A Matrix-Isolation FTIR and Theoretical Study. *J. Phys. Chem. A* **2002**, *106*, 3077–3083.

- (24) Beach, D. B.; Jasinski, J. M. Excimer Laser Photochemistry of Silane–Ammonia Mixtures at 193 nm. *J. Phys. Chem.* **1990**, *94*, 3019–3026.

- (25) Lattanzi, V.; McCarthy, M. C.; Thaddeus, P.; Thorwirth, S. 65th International Symposium On Molecular Spectroscopy; Columbus, OH, 2010.

- (26) Johnson, D. R.; Lovas, F. J. Microwave Detection of the Molecular Transient Methyleneimine ($\text{CH}_2 = \text{NH}$). *Chem. Phys. Lett.* **1972**, *15*, 65–68.
- (27) Polce, M. J.; Kim, Y.; Wesdemiotis, C. First Experimental Characterization of Aminocarbene. *Int. J. Mass Spectrom. Ion Processes* **1997**, *167*, 309–315.
- (28) Balucani, N.; Bergeat, A.; Cartechini, L.; Volpi, G. G.; Casavecchia, P.; Skouteris, D.; Rosi, M. Combined Crossed Molecular Beam and Theoretical Studies of the $\text{N}(^2\text{D}) + \text{CH}_4$ Reaction and Implications for Atmospheric Models of Titan. *J. Phys. Chem. A* **2009**, *113*, 11138–11152.
- (29) Blitz, M. A.; Talbi, D.; Seakins, P. W.; Smith, I. W. M. Rate Constants and Branching Ratios for the Reaction of CH Radicals with NH_3 : A Combined Experimental and Theoretical Study. *J. Phys. Chem. A* **2012**, *116*, 5877–5885.
- (30) Levine, R. D. *Molecular Reaction Dynamics*; Cambridge University Press: Cambridge, 2005.
- (31) Vernon, M. F. *Molecular Beam Scattering*. Ph.D. Thesis, University of California: Berkeley, CA, 1983.
- (32) Gu, X.; Guo, Y.; Zhang, F.; Mebel, A. M.; Kaiser, R. I. Reaction Dynamics of Carbon-Bearing Radicals in Circumstellar Envelopes of Carbon Stars. *Faraday Discuss.* **2006**, *133*, 245–275.
- (33) Miller, W. B.; Safron, S. A.; Herschbach, D. R. Exchange Reactions of Alkali Atoms with Alkali Halides: A Collision Complex Mechanism. *Discuss. Faraday Soc.* **1967**, *44*, 108–122.
- (34) Chen, W.-K.; Lu, I.-C.; Chaudhuri, C.; Huang, W.-J.; Lee, S.-H. Investigations of Silicon- Nitrogen Hydrides from Reaction of Nitrogen Atoms with Silane: Experiments and Calculations. *J. Phys. Chem. A* **2008**, *112*, 8479–8486.
- (35) Lu, I.-C.; Chen, W.-K.; Chaudhuri, C.; Huang, W.-J.; Lin, J. J.; Lee, S.-H. Exploring the Dynamics of Reaction $\text{N} + \text{SiH}_4$ with Crossed Molecular-Beam Experiments and Quantum-Chemical Calculations. *J. Chem. Phys.* **2008**, *129*, 174304.
- (36) Jursic, B. S. Quadratic Complete Basis Set Ab Initio and Hybrid Density Functional Theory Studies of the Stability of HNC, HCN, H_2NCH and HNCH_2 , Their Isomerizations, and the Hydrogen Insertion Reactions for HCN and HNC. *J. Chem. Soc., Faraday Trans.* **1997**, *93*, 2355–2359.
- (37) Gong, S.; Wang, C.; Li, Q. Theoretical Study of the Mechanisms and Rate Constants on the Reaction of H_2CNH with $\text{O}(^3\text{P})$. *Comput. Theor. Chem.* **2012**, *991*, 141–149.
- (38) Eckhardt, A. K.; Schreiner, P. R. Spectroscopic Evidence for Aminomethylene ($\text{H}-\text{C}-\text{NH}_2$) — the Simplest Amino Carbene. *Angew. Chem., Int. Ed.* **2018**, *57*, 5248–5252.
- (39) Bourgalais, J.; Caster, K. L.; Durif, O.; Osborn, D. L.; Le Picard, S. D.; Goulay, F. Product Detection of the CH Radical Reactions with Ammonia and Methyl-Substituted Amines. *J. Phys. Chem. A* **2019**, *123*, 2178–2193.
- (40) Jursic, B. S. Density Functional Theory and Quadratic Complete Basis Set Ab Initio Studies of the HNSi to HSiN Isomerization and Hydrogen Insertion Reactions with Further Isomerizations of the Insertion Products. *J. Mol. Struct.: THEOCHEM* **1999**, *460*, 11–18.
- (41) Kaiser, R. I.; Maksyutenko, P.; Ennis, C.; Zhang, F.; Gu, X.; Krishtal, S. P.; Mebel, A. M.; Kostko, O.; Ahmed, M. Untangling the Chemical Evolution of Titan's Atmosphere and Surface—from Homogeneous to Heterogeneous Chemistry. *Faraday Discuss.* **2010**, *147*, 429–478.
- (42) Yang, Z.; Sun, B.-J.; He, C.; Goettl, S.; Lin, Y.-T.; Chang, A. H. H.; Kaiser, R. I. Combined Experimental and Computational Study on the Reaction Dynamics of the D1-Silyliidyne (SiD)–Silane (SiH_4) System. *J. Phys. Chem. A* **2021**, *125*, 2472–2479.
- (43) Bauer, W.; Becker, K. H.; Düren, R.; Hubrich, C.; Meuser, R. Radiative Lifetime Measurements of SiH ($A^2\Delta$) by Laser-Induced Fluorescence. *Chem. Phys. Lett.* **1984**, *108*, 560–561.
- (44) Daly, N. R. Scintillation Type Mass Spectrometer Ion Detector. *Rev. Sci. Instrum.* **1960**, *31*, 264–267.
- (45) Brink, G. O. Electron Bombardment Molecular Beam Detector. *Rev. Sci. Instrum.* **1966**, *37*, 857–860.
- (46) Weiss, P. S. *Reaction Dynamics of Electronically Excited Alkali Atoms with Simple Molecules*. Ph.D. Thesis, University of California, Berkeley, CA, 1986.
- (47) Kaiser, R. I.; Ochsenfeld, C.; Stranges, D.; Head-Gordon, M.; Lee, Y. T. Combined Crossed Molecular Beams and Ab Initio Investigation of the Formation of Carbon-Bearing Molecules in the Interstellar Medium via Neutral–Neutral Reactions. *Faraday Discuss.* **1998**, *109*, 183–204.
- (48) Becke, A. D. Density-Functional Thermochemistry. III. The Role of Exact Exchange. *J. Chem. Phys.* **1993**, *98*, 5648–5652.
- (49) Lee, C.; Yang, W.; Parr, R. G. Development of the Colle-Salvetti Correlation-Energy Formula into a Functional of the Electron Density. *Phys. Rev. B: Condens. Matter Mater. Phys.* **1988**, *37*, 785–789.
- (50) Grimme, S. Semiempirical Hybrid Density Functional with Perturbative Second-Order Correlation. *J. Chem. Phys.* **2006**, *124*, 034108.
- (51) Goerigk, L.; Grimme, S. Efficient and Accurate Double-Hybrid-Meta-GGA Density Functionals-Evaluation with the Extended GMTKN30 Database for General Main Group Thermochemistry, Kinetics, and Noncovalent Interactions. *J. Chem. Theory Comput.* **2011**, *7*, 291–309.
- (52) Grimme, S.; Ehrlich, S.; Goerigk, L. Effect of the Damping Function in Dispersion Corrected Density Functional Theory. *J. Comput. Chem.* **2011**, *32*, 1456–1465.
- (53) Cížek, J. In *Advances in Chemical Physics*, Vol. 14; Hariharan, P. C., Ed.; Wiley Interscience: New York, 1969.
- (54) Purvis, G. D.; Bartlett, R. J. A Full Coupled-Cluster Singles and Doubles Model: The Inclusion of Disconnected Triples. *J. Chem. Phys.* **1982**, *76*, 1910–1918.
- (55) Scuseria, G. E.; Janssen, C. L.; Schaefer, H. F. III An Efficient Reformulation of the Closed-Shell Coupled Cluster Single and Double Excitation (CCSD) Equations. *J. Chem. Phys.* **1988**, *89*, 7382–7387.
- (56) Scuseria, G. E.; Schaefer, H. F. III Is Coupled Cluster Singles and Doubles (CCSD) More Computationally Intensive Than Quadratic Configuration Interaction (QCISD)? *J. Chem. Phys.* **1989**, *90*, 3700–3703.
- (57) Adler, T. B.; Knizia, G.; Werner, H.-J. A simple and efficient CCSD(T)-F12 approximation. *J. Chem. Phys.* **2007**, *127*, 221106.
- (58) Knizia, G.; Adler, T. B.; Werner, H.-J. Simplified CCSD(T)-F12 Methods: Theory and Benchmarks. *J. Chem. Phys.* **2009**, *130*, 054104.
- (59) Dunning Jr, T. H. Gaussian Basis Sets for Use in Correlated Molecular Calculations. I. The Atoms Boron through Neon and Hydrogen. *J. Chem. Phys.* **1989**, *90*, 1007–1023.
- (60) Martin, J. M. L.; Uzan, O. Basis Set Convergence in Second-Row Compounds. The Importance of Core Polarization Functions. *Chem. Phys. Lett.* **1998**, *282*, 16–24.
- (61) Hill, J. G.; Mazumder, S.; Peterson, K. A. Correlation Consistent Basis Sets for Molecular Core-Valence Effects with Explicitly Correlated Wave Functions: The Atoms B–Ne and Al–Ar. *J. Chem. Phys.* **2010**, *132*, 054108.
- (62) Barone, V. Anharmonic Vibrational Properties by a Fully Automated Second-Order Perturbative Approach. *J. Chem. Phys.* **2005**, *122*, 014108.
- (63) Frisch, M. J.; Trucks, G. W.; Schlegel, H. B.; Scuseria, G. E.; Robb, M. A.; Cheeseman, J. R.; Scalmani, G.; Barone, V.; Mennucci, B.; Petersson, G. A. et al. *Gaussian 09*, revision D. 01; Gaussian Inc.: Wallingford, CT, 2009.
- (64) Werner, H. J.; Knowles, P. J.; Knizia, G.; Manby, F. R.; Schütz, M.; Celani, P.; Korona, T.; Lindh, R.; Mitrushenkov, A.; Rauhut, G. *MOLPRO*, version 2010.1 A Package of Ab Initio Programs; University of Cardiff: Cardiff, U.K., 2010.